Journal of Sound and Vibration (2002) **254**(2), 313–325
doi:10.1006/jsvi.2001.4097, available online at http://www.idealibrary.com on IDEAL®

NEW NON-LINEAR MODELLING FOR VIBRATION ANALYSIS OF A STRAIGHT PIPE CONVEYING FLUID

S. I. Lee and J. Chung

Department of Mechanical Engineering, Hanyang University, 1271 *Sa*-1-*dong*, *Ansan*, *Kyunggi-do* 425-791, *Republic of Korea. E-mail*: *jchung@hanyang.ac.kr*

(*Received* 27 *March* 2001, *and in final form* 28 *October* 2001)

A new non-linear model of a straight pipe conveying fluid is presented for vibration analysis when the pipe is fixed at both ends. Using the Euler–Bernoulli beam theory and the non-linear Lagrange strain theory, from the extended Hamilton's principle the coupled non-linear equations of motion for the longitudinal and transverse displacements are derived. These equations of motion are discretized by using the Galerkin method. After the discretized equations are linearized in the neighbourhood of the equilibrium position, the natural frequencies are computed from the linearized equations. On the other hand, the time histories for the displacements are also obtained by applying the generalized-α time integration method to the non-linear discretized equations. The validity of the new modelling is provided by comparing results from the proposed non-linear equations with those from the equations proposed by Païdoussis.

1. INTRODUCTION

Vibration of a pipe conveying fluid is an important problem that needs to be resolved in refrigerators, air-conditioners, chemical plants, hydropower systems and so on. Therefore, vibration analysis of a pipe vibration has been a subject of numerous investigations due to their wide application in many industrial fields. Many researchers [1–7] presented studies on modelling and derivation of the equations of motion for pipes conveying fluid. They carried out the vibration and stability analysis of straight or curved pipes subjected to various supports or loading. In particular, comprehensive reviews on various pipe modelling and analysis are given in a book written by Païdoussis [1]. In recent years, some studies carried out non-linear formulations and analyses of pipes conveying fluid [6, 7]. Most of the previous non-linear equations were derived not only by using the order-of-magnitude approximation but also by considering non-linearity and the infinitesimal strain simultaneously [1, 2, 6, 7]. However, it is more reasonable that non-linearity should be considered in the general non-linear Lagrange strain that is often called the von Karman strain. The reason for this is that the infinitesimal strain theory is suitable for a linear system while the general Lagrange strain is more suitable for a non-linear system [8].

In this study, a new non-linear model of straight pipe conveying fluid is presented for vibration analysis when the pipe is fixed at both ends. The main difference between the linear and the non-linear models is that the transverse displacement is coupled with the longitudinal displacement through the non-linear terms. In order to take the effects of non-linearity into account, the general Lagrange strain theory is adopted instead of the conventional infinitesimal strain theory. On the other hand, it is assumed that the pipe is treated as the Euler–Bernoulli beam and it has linear relations between the stresses and the

0022-460X/02/$35.00

displacements. Based on the above background, coupled non-linear equations of motion are derived for the longitudinal and transverse displacements from the extended Hamilton principle [9]. After the equations are discretized by the Galerkin method and then linearized in the neighbourhood of the equilibrium position, the natural frequencies for the transverse vibrations are computed and verified. Furthermore, the non-linear dynamic responses, i.e., the time histories of the displacements are computed by using the generalized-time integration method [10]. Finally, the computation results from the proposed non-linear equations are compared with those from the equations proposed by Païdoussis and his co-workers [1, 6].

2. EQUATIONS OF MOTION

Consider an extensible straight pipe with uniform internal flow and harmonic external excitation, as shown in Figure 1. The straight pipe, clamped at both ends, has dimensions given by the length L, the cross-sectional outer diameter d_o and the thickness h. If it is assumed that the pipe is sufficiently slender, that is, $d_o/L < 0{\cdot}1$, it can be modelled as the Euler–Bernoulli beam. Moreover, the fluid in the pipe is assumed to be incompressible so that its velocity is uniform inside the pipe. This means that so-called "plug-flow" is assumed, where the secondary flow effects are negligible [1]. Therefore, it is reasonable that the axial velocity $U(t)$ and the acceleration $\dot{U}(t)$ are uniform in the pipe.

In order to consider the non-linearity of the pipe, in this paper, the general Lagrange strain theory is used along with the Euler–Bernoulli beam theory. Since the pipe is modelled as the Euler–Bernoulli beam, the displacements in the x and y directions, $u_x(x, y, t)$ and $u_y(x, y, t)$, for a point of the pipe may be expressed by

$$u_x(x, y, t) = u(x, t) - y\frac{\partial v(x, t)}{\partial x}, \quad u_y(x, y, t) = v(x, t), \tag{1}$$

where $u(x, t)$ and $v(x, t)$ are the longitudinal and transverse displacements of a point on the centre line of the pipe respectively. The displacements and strains of the pipe may not be

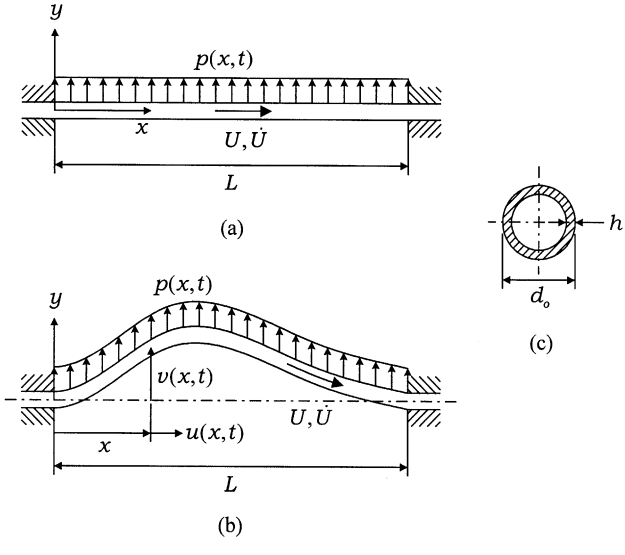

Figure 1. Schematics of a straight pipe conveying fluid when both ends are fixed: (a) the pipe before deformation; (b) the pipe after deformation; and (c) the cross-section of the pipe.

small, so that the longitudinal displacement as well as the transverse displacement is included in the formulation. The non-linearity of the pipe can be considered by the Lagrange strain–displacement relations, which provide the relations between the strains and displacements:

$$\varepsilon_x = \frac{\partial u_x}{\partial x} + \frac{1}{2}\left(\frac{\partial u_x}{\partial x}\right)^2 + \frac{1}{2}\left(\frac{\partial u_y}{\partial x}\right)^2, \qquad \varepsilon_y = \frac{\partial u_y}{\partial y} + \frac{1}{2}\left(\frac{\partial u_x}{\partial y}\right)^2 + \frac{1}{2}\left(\frac{\partial u_y}{\partial y}\right)^2,$$

$$\varepsilon_{xy} = \frac{1}{2}\left(\frac{\partial u_y}{\partial x} + \frac{\partial u_x}{\partial y} + \frac{\partial u_x}{\partial x}\frac{\partial u_x}{\partial y} + \frac{\partial u_y}{\partial x}\frac{\partial u_y}{\partial y}\right), \tag{2}$$

where ε_x and ε_y are the longitudinal and transverse normal strains, and ε_{xy} is the shear strain. Substitution of equations (1) into equations (2) leads to

$$\varepsilon_x = u' + \tfrac{1}{2}(u'^2 + v'^2) - y(1 + u')v'' + \tfrac{1}{2}y^2 v''^2, \qquad \varepsilon_y = \tfrac{1}{2}v'^2, \quad \varepsilon_{xy} = -\tfrac{1}{2}u'v' + \tfrac{1}{2}yv'v'', \tag{3}$$

where the superposed prime represents differentiation with respect to x. Note again that the non-linear terms in equations (3) originate from the non-linearity of the pipe due to the large deformation.

Consider the difference of the non-linear strain–displacement relations between the proposed modelling and the conventional modelling [1, 2, 6, 7]. Païdoussis and his co-workers [1, 6, 7] and Thurman and Mote [2] used the approximated non-linear strain–displacement relations given by

$$\varepsilon = \sqrt{(1 + u')^2 + v'^2} - 1, \quad \kappa = \sqrt{u''^2 + v''^2}, \tag{4}$$

where ε and κ are the axial strain and the curvature of the pipe respectively. These non-linear relations are derived by considering the non-linearity and the infinitesimal strains simultaneously. In other words, to consider the non-linearity, the non-linear strains are obtained by applying the Pythagorean theorem to the infinitesimal strains. However, it is reasonable that the non-linearity is considered in the general Lagrangian strain theory that is often called the von Karman strain theory, because the infinitesimal strain theory is suitable for a linear system while the von Karman strain theory is suitable for a non-linear system [8]. Moreover, the order-of-magnitude approximation was used when the other researchers derived non-linear equations of motion. Consequently, compared to the strains of equations (4), the non-linear strains of this study given by equations (3) are consistently derived from the general Lagrange strain theory that permits large displacements and strains.

Next, consider the stress–strain relation in the pipe. It is assumed that the material of the pipe is homogeneous, isotropic, elastic and Hoken. Since the pipe is slender and the thickness h is small compared to other dimensions, the axial stress σ_x can be represented by

$$\sigma_x = E\varepsilon_x^L, \tag{5}$$

where E is Young's modulus and ε_x^L is the linearized axial strain. The linearized strains ε_x^L, ε_y^L and ε_{xy}^L are obtained by linearization of the strains given by equations (3):

$$\varepsilon_x^L = u' - yv'', \quad \varepsilon_y^L = \varepsilon_{xy}^L = 0. \tag{6}$$

Hence, in this modelling, the non-linear strains and the linear stresses are used to obtain the equations of motion. A more detailed discussion of this kind of modelling can be found in

Chung *et al.* [11]; furthermore, this modelling technique is applied to derive the equations of motion for an axially moving string [12].

Under the assumptions described above, the strain energy of the pipe conveying fluid is given by

$$P = \frac{1}{2}\int_V \sigma_x \varepsilon_x \, \mathrm{d}V, \tag{7}$$

where V is the volume of the pipe. Substituting equations (3) and (5) into equation (7), the strain energy can be expressed as

$$P = \frac{1}{2} EA \int_0^L \left[u'^2 + \frac{1}{2} u'(u'^2 + v'^2) \right] \mathrm{d}x + \frac{1}{2} EI \int_0^L \left(1 + \frac{3}{2} u' \right) v''^2 \, \mathrm{d}x, \tag{8}$$

where A is the cross-sectional area of the pipe and I is the area moment of inertia.

To obtain the kinetic energy of the pipe conveying fluid, consider not only the velocity of fluid along the pipe but also the velocity of the pipe. First, the displacement vector of a point on the centre line of the deformed pipe can be written as

$$\mathbf{r} = u\,\mathbf{i} + v\,\mathbf{j}, \tag{9}$$

where $\mathbf{i}$ and $\mathbf{j}$ are the unit vectors in the x and y directions respectively. Then, the pipe velocity $\mathbf{v}_p$ and the fluid velocity along the pipe $\mathbf{v}_f$ are given by

$$\mathbf{v}_p = \dot{u}\,\mathbf{i} + \dot{v}\,\mathbf{j}, \quad \mathbf{v}_f = [\dot{u} + U(1 + u')]\mathbf{i} + (\dot{v} + Uv')\mathbf{j}, \tag{10}$$

where the superposed dot stands for differentiation with respect to time. The fluid velocity $\mathbf{v}_f$ is obtained from the material derivative of $\mathbf{r}$ with respect to time. Neglecting the rotary inertia effect and the secondary flow effect, the kinetic energy for the pipe conveying fluid is given by

$$K = \frac{1}{2A}\int_V (m_p \mathbf{v}_p \cdot \mathbf{v}_p + m_f \mathbf{v}_f \cdot \mathbf{v}_f) \, \mathrm{d}V, \tag{11}$$

where m_p and m_f are the mass densities of the pipe and the fluid per unit pipe length respectively. Substituting equations (10) into equation (11), the kinetic energy is expressed as

$$K = \frac{1}{2} m_p \int_0^L (\dot{u}^2 + \dot{v}^2) \, \mathrm{d}x + \frac{1}{2} m_f \int_0^L \{[\dot{u} + U(1 + u')]^2 + (\dot{v} + Uv')^2\} \, \mathrm{d}x. \tag{12}$$

The equations of motions of the pipe with fluid transport and the corresponding boundary conditions are obtained from the extended Hamilton principle [9]. The extended Hamilton principle may be described as

$$\int_{t_1}^{t_2} (\delta K - \delta P + \delta W_{nc} - \delta M) \, \mathrm{d}t = 0, \tag{13}$$

where δ is the variation operator, δW_{nc} is the virtual work done by the non-conservative forces and δM is the virtual momentum change. These two quantities for the pipe conveying

fluid, shown in Figure 1, are given by

$$\delta W_{nc} = \int_0^L p(x,t)\delta v \, \mathrm{d}x, \quad \delta M = [m_f(\mathbf{v}_f \cdot \delta \mathbf{r})(U\,\mathbf{i}\cdot\mathbf{n})]_0^L, \tag{14}$$

where $p(x, t)$ is the transverse load per unit length of the pipe and $\mathbf{n}$ is the outward normal vector at the boundaries. Introducing equations (8), (12) and (14) into equation (13), the coupled non-linear equations of motion for the pipe conveying fluid are derived as follows:

$$(m_p + m_f)\ddot{u} + m_f\dot{U}(1+u') + 2m_fU\dot{u}' + m_fU^2u'' - EA(u'' + \tfrac{3}{2}u'u'' + \tfrac{1}{2}v'v'') - \tfrac{3}{2}EIv''v^{(3)} = 0, \tag{15}$$

$$(m_p + m_f)\ddot{v} + m_f\dot{U}v' + 2m_fU\dot{v}' + m_fU^2v'' - \tfrac{1}{2}EA(u''v' + u'v'') + EI(v^{(4)} + \tfrac{3}{2}u'v^{(4)} + 3u''v^{(3)} + \tfrac{3}{2}u^{(3)}v'') = p. \tag{16}$$

The associated boundary conditions are given by

$$u = v = v' = 0 \quad \text{at } x = 0, L. \tag{17}$$

It needs to be emphasized that the above equations are derived by adopting the non-linear Lagrange strains and linearized stresses in order to consider the non-linearity of the pipe.

It is interesting to check as to what is the difference between the newly proposed equations and the previously presented equations. Since the equations derived by Thurman and Mote [2] are simplified forms of the equations presented by Païdoussis and his co-workers [1, 6, 7], the equations proposed in this paper are compared with the equations of Païdoussis and his co-workers. Using the same notations of this paper, the equations of Païdoussis and his co-workers can be rewritten as

$$(m_p + m_f)\ddot{u} + m_f\dot{U}(1+u') + 2m_fU\dot{u}' + m_fU^2u'' - EA(u'' + v'v'') - EI(v'v^{(4)} + v''v^{(3)}) = 0, \tag{18}$$

$$(m_p + m_f)\ddot{v} + m_f\dot{U}v' + 2m_fU\dot{v}' + m_fU^2v'' - EA(u''v' + u'v'' + \tfrac{3}{2}v'^2v'') + EI(v^{(4)} - 2u'v^{(4)} - 4u''v^{(3)} - 3u^{(3)}v'' - u^{(4)}v' - 2v'^2v^{(4)} - 8v'v''v^{(3)} - 2v''^2) = p. \tag{19}$$

The main difference of equations (16) and (17) from equations (18) and (19) is shown in non-linear terms. On the other hand, as expected, the linear terms are the same in both equations of motion.

3. DISCRETIZED EQUATIONS OF MOTION

Approximate solutions for the discretized equations can be found in a finite-dimensional function space. The longitudinal and transverse displacements may be represented by the trial functions that are expressed as a series of the basis functions:

$$u(x,t) = \sum_{n=0}^{N} U_n(x)T_n^u(t), \quad v(x,t) = \sum_{n=0}^{N} V_n(x)T_n^v(t), \tag{20}$$

where N is the total number of the basis functions, $U_n(x)$ and $V_n(x)$ are the comparison functions, and $T_n^u(t)$ and $T_n^v(t)$ are unknown functions of time to be determined. The weighting functions corresponding to the trial functions are given by

$$\bar{u}(x,t) = \sum_{n=0}^{N} U_n(x)\,\bar{T}_n^u(t), \quad \bar{v}(x,t) = \sum_{n=0}^{N} V_n(x)\,\bar{T}_n^v(t), \tag{21}$$

where $\bar{T}_n^u(t)$ and $\bar{T}_n^v(t)$ are arbitrary functions of time. If the comparison functions for the longitudinal and transverse displacements are chosen as

$$U_n(x) = a_n x^{n+1}(L-x), \quad V_n(x) = b_n x^{n+2}(L-x)^2, \tag{22}$$

in which a_n and b_n are arbitrary constants, they automatically satisfy all the boundary conditions given by equation (17). Meanwhile, the coefficients a_n and b_n can be determined by the normalization conditions

$$\int_0^L U_n\,\mathrm{d}x = \int_0^L V_n\,\mathrm{d}x = 1. \tag{23}$$

The equations of motion derived in the previous section are discretized by the Galerkin method. Substituting u and v from equations (20) into equations (15) and (16), multiplying these equations by $\bar{u}$ and $\bar{v}$ from equations (21), respectively, summing all the equations, integrating them over the length L, and then collecting all the terms with respect to $\bar{T}_n^u(t)$ and $\bar{T}_n^v(t)$, the coefficients of $\bar{T}_n^u(t)$ and $\bar{T}_n^v(t)$ provide the discretized equations given by

$$\sum_{n=0}^{N}\left[m_{mn}^u \ddot{T}_n^u + 2Ug_{mn}^u \dot{T}_n^u + (k_{mn}^u + U^2 h_{mn}^u + \dot{U} g_{mn}^u) T_n^u + \sum_{j=0}^{N} (\alpha_{jmn}^u T_j^u T_n^u + \alpha_{jmn}^v T_j^v T_n^v)\right]$$

$$= f_m^u, \quad m = 0, 1, \ldots, N, \tag{24}$$

$$\sum_{n=0}^{N}\left[m_{mn}^v \ddot{T}_n^v + 2Ug_{mn}^v \dot{T}_n^v + (k_{mn}^v + U^2 h_{mn}^v + \dot{U} g_{mn}^v) T_n^v + \sum_{j=0}^{N} \alpha_{jmn}^{uv} T_j^u T_n^v\right] = f_m^v,$$

$$m = 0, 1, \ldots, N, \tag{25}$$

where

$$m_{mn}^u = (m_p + m_f)\int_0^L U_m U_n\,\mathrm{d}x, \quad m_{mn}^v = (m_p + m_f)\int_0^L V_m V_n\,\mathrm{d}x, \; g_{mn}^u = m_f \int_0^L U_m \frac{\mathrm{d}U_n}{\mathrm{d}x}\mathrm{d}x,$$

$$g_{mn}^v = m_f \int_0^L V_m \frac{\mathrm{d}V_n}{\mathrm{d}x}\mathrm{d}x, \; h_{mn}^u = m_f \int_0^L U_m \frac{\mathrm{d}^2 U_n}{\mathrm{d}x^2}\mathrm{d}x, \quad h_{mn}^v = m_f \int_0^L V_m \frac{\mathrm{d}^2 V_n}{\mathrm{d}x^2}\mathrm{d}x,$$

$$k_{mn}^u = -EA\int_0^L U_m \frac{\mathrm{d}^2 U_n}{\mathrm{d}x^2}\mathrm{d}x, \quad k_{mn}^v = EI\int_0^L V_m \frac{\mathrm{d}^4 V_n}{\mathrm{d}x^4}\mathrm{d}x, \; \alpha_{jmn}^u = -\frac{3}{2}EA\int_0^L U_m \frac{\mathrm{d}U_j}{\mathrm{d}x}\frac{\mathrm{d}^2 U_n}{\mathrm{d}x^2}\mathrm{d}x,$$

$$\alpha_{jmn}^v = -\frac{1}{2}EA\int_0^L U_m \frac{\mathrm{d}V_j}{\mathrm{d}x}\frac{\mathrm{d}^2 V_n}{\mathrm{d}x^2}\mathrm{d}x - \frac{3}{2}EI\int_0^L U_m \frac{\mathrm{d}V_j}{\mathrm{d}x}\frac{\mathrm{d}^3 V_n}{\mathrm{d}x^3}\mathrm{d}x,$$

$$\alpha_{jmn}^{uv} = -\frac{1}{2}EA\int_0^L V_m \frac{\mathrm{d}}{\mathrm{d}x}\left(\frac{\mathrm{d}U_j}{\mathrm{d}x}\frac{\mathrm{d}V_n}{\mathrm{d}x}\right)\mathrm{d}x$$

$$+\frac{3}{2}EI\int_0^L V_m\left(\frac{\mathrm{d}U_j}{\mathrm{d}x}\frac{\mathrm{d}^4V_n}{\mathrm{d}x^4} + 2\frac{\mathrm{d}^2U_j}{\mathrm{d}x^2}\frac{\mathrm{d}^3V_n}{\mathrm{d}x^3} + \frac{\mathrm{d}^3U_j}{\mathrm{d}x^3}\frac{\mathrm{d}^2V_n}{\mathrm{d}x^2}\right)\mathrm{d}x,$$

$$f_m^u = m_f\dot{U}\int_0^L U_m\,\mathrm{d}x, \quad f_m^v = \int_0^L V_m p\,\mathrm{d}x. \tag{26}$$

Equations (24) and (25) can be rewritten in vector–matrix form as

$$\mathbf{M}\ddot{\mathbf{T}}(t) + 2U\mathbf{G}\dot{\mathbf{T}}(t) + (\mathbf{K} + U^2\mathbf{H} + \dot{U}\mathbf{G})\mathbf{T}(t) + \mathbf{N}(\mathbf{T}(t)) = \mathbf{F}(t), \tag{27}$$

where $\mathbf{M}$ is the mass matrix, $\mathbf{G}$ is the matrix related to the gyroscopic force, $\mathbf{K}$ is the structural stiffness matrix, $\mathbf{H}$ is the matrix related to the centrifugal force for the fluid, $\mathbf{N}(\mathbf{T}(t))$ is the non-linear internal force vector, $\mathbf{F}(t)$ is the external force vector and $\mathbf{T}$ is given by

$$\mathbf{T} = \{T_0^u, T_1^u, \ldots, T_N^u, T_0^v, T_1^v, \ldots, T_N^v\}^{\mathrm{T}}. \tag{28}$$

4. NATURAL FREQUENCIES

The discretized equations of motion can be verified by computing the natural frequencies of the pipe. To do this, it is necessary to obtain the linearized equations of motion in the neighbourhood of the equilibrium position. When the pipe is in the steady state and the external force is neglected, the linearized equation of equation (27) is given by

$$\mathbf{M}\ddot{\mathbf{T}}(t) + 2U\mathbf{G}\dot{\mathbf{T}}(t) + (\mathbf{K} + U^2\mathbf{H})\mathbf{T}(t) = \mathbf{0}. \tag{29}$$

In order to find the natural frequencies from equation (29), it is convenient to transform equation (29) into

$$\mathbf{A}\dot{\mathbf{Y}}(t) + \mathbf{B}\mathbf{Y}(t) = \mathbf{0}, \tag{30}$$

where

$$\mathbf{A} = \begin{bmatrix}\mathbf{0} & \mathbf{I}\\ \mathbf{M} & \mathbf{0}\end{bmatrix}, \ \mathbf{B} = \begin{bmatrix}-\mathbf{I} & \mathbf{0}\\ 2U\mathbf{G} & \mathbf{K} + U^2\mathbf{H}\end{bmatrix}, \ \mathbf{Y}(t) = \begin{Bmatrix}\dot{\mathbf{T}}(t)\\ \mathbf{T}(t)\end{Bmatrix}. \tag{31}$$

Assuming the solution of equation (30) as $\mathbf{Y}(t) = \mathbf{Y}_0 e^{\lambda_n t}$, the complex eigenvalue λ_n can be computed from

$$\det(\mathbf{B} + \lambda_n\mathbf{A}) = 0. \tag{32}$$

Consider the convergence characteristics of the natural frequencies for the pipe. If there is no specification, the material properties used in the computation of this study are given by $m_p = 0{\cdot}05636$ kg/m, $m_f/(m_p + m_f) = 0{\cdot}1$, $E = 10 \times 10^9$ Pa, $L = 2{\cdot}0$ m, $d_o = 20$ mm and $h = 0{\cdot}1$ mm. Table 1 shows the convergence characteristics of the natural frequencies with the number of basis functions N when the pipe is stationary, i.e., $U = \dot{U} = 0$. It is obvious that, as N increases, the computed natural frequencies approach the exact values presented by Blevins [13]. Another verification for the convergence of the natural frequencies is

TABLE 1

Convergence characteristics of the natural frequencies (rad/s) when $U = \dot{U} = 0$

	Transverse vibration			Longitudinal vibration		
N	First	Second	Third	First	Second	Third
1	131·84	369·57	N/A	5252·81	10765·0	N/A
2	131·40	369·57	749·56	5218·49	10765·0	16786·8
3	131·40	362·31	749·56	5218·49	10440·0	16786·8
4	131·40	362·31	711·38	5218·45	10440·0	15685·9
5	131·40	362·19	711·38	5218·45	10436·9	15685·9
6	131·40	362·19	710·06	5218·45	10436·9	15655·6
Exact [13]	131·39	362·19	710·04	5218·40	10436·4	15653·5

TABLE 2

Convergence characteristics of the natural frequencies (rad/s) when $U = 15{\cdot}0$ *m/s and* $\dot{U} = 0$

	Transverse vibration			Longitudinal vibration		
N	First	Second	Third	First	Second	Third
1	48·206	295·92	N/A	5251·5	10762·8	N/A
2	38·288	291·86	680·41	5217·2	10762·5	16783·6
3	38·172	276·50	675·22	5217·2	10437·4	16783·2
4	38·070	275·78	625·28	5217·2	10437·4	15682·3
5	38·069	275·46	623·20	5217·2	10434·3	15682·1
6	38·069	275·46	621·11	5217·2	10434·3	15651·7
7	38·069	275·44	621·01	5217·2	10434·3	15651·7

provided when the fluid has a constant velocity. As seen in Table 2, when $U = 15{\cdot}0$ m/s and $\dot{U} = 0$, the computed natural frequencies converge with the number of basis functions N.

The discretized equations are also verified by investigating the variation of the complex eigenvalue with the fluid velocity. For comparison of the computation results, it is convenient to introduce the dimensionless eigenvalue $\bar{\lambda}_n$ and the dimensionless fluid velocity $\bar{U}$ given by

$$\bar{\lambda}_n = \lambda_n L^2 \sqrt{\frac{m_p + m_f}{EI}}, \quad \bar{U} = UL \sqrt{\frac{m_f}{EI}}. \tag{33}$$

When $\dot{U} = 0$, the variation of the dimensionless eigenvalues versus the dimensionless fluid velocity is illustrated in Figure 2, where the imaginary part of the eigenvalue represents the natural frequency of the pipe. This plot is nearly the same as that presented by Païdoussis [1]. It is well known that the pipe becomes unstable if at least one of the eigenvalues has a positive real part. As shown in Figure 2, the critical fluid velocity computed from equation (32) is $\bar{U}_c = 6{\cdot}28$, which is the same as the critical velocity $\bar{U}_c = 2\pi$ given by Païdoussis [1]. In the region of $6{\cdot}28 < \bar{U} < 8{\cdot}99$, the first mode has real eigenvalues, which incur the divergence instability. However, when $\bar{U} > 8{\cdot}99$, the first and second modes are combined and they produce the same eigenvalues that have the imaginary parts as well as the real parts. Therefore, the velocity region of $\bar{U} > 8{\cdot}99$ is related to the flutter instability.

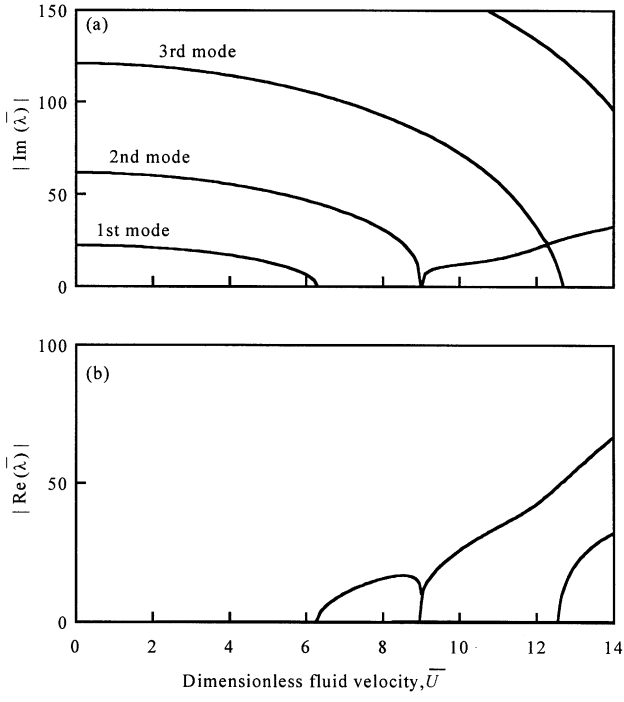

Figure 2. Variation of the complex eigenvalues for the dimensionless fluid velocity: (a) the imaginary part; and (b) the real part.

5. DYNAMIC RESPONSES

From the discretized non-linear equation of motion given by equation (27), the time histories of the displacements are obtained by the generalized-α time integration method [10]. To apply the generalized-α method, it is convenient to express the discretized equation (27) as

$$\mathbf{M}\mathbf{a}_{n+1-\alpha_m} + 2U_{n+1-\alpha_f}\mathbf{G}\mathbf{v}_{n+1-\alpha_f} + (\mathbf{K} + U^2_{n+1-\alpha_f}\mathbf{H} + \dot{U}_{n+1-\alpha_f}\mathbf{G})\mathbf{d}_{n+1-\alpha_f} + \mathbf{N}(\mathbf{d}_{n+1-\alpha_f}) = \mathbf{F}_{n+1-\alpha_f}, \tag{34}$$

where

$$\mathbf{d}_{n+1-\alpha_f} = (1-\alpha_f)\mathbf{d}_{n+1} + \alpha_f\mathbf{d}_n,\ \mathbf{v}_{n+1-\alpha_f} = (1-\alpha_f)\mathbf{v}_{n+1} + \alpha_f\mathbf{v}_n,\ \mathbf{a}_{n+1-\alpha_m} = (1-\alpha_m)\mathbf{a}_{n+1} + \alpha_m\mathbf{a}_n,$$

$$\mathbf{F}_{n+1-\alpha_f} = \mathbf{F}(t_{n+1-\alpha_f}),\ U_{n+1-\alpha_f} = U(t_{n+1-\alpha_f}),\ \dot{U}_{n+1-\alpha_f} = \dot{U}(t_{n+1-\alpha_f}),$$

$$t_{n+1-\alpha_f} = (1-\alpha_f)t_{n+1} + \alpha_f t_n, \tag{35}$$

and

$$\mathbf{d}_{n+1} = \mathbf{d}_n + \Delta t\mathbf{v}_n + (1/2-\beta)\Delta t^2\mathbf{a}_n + \beta\Delta t^2\mathbf{a}_{n+1},\ \mathbf{v}_{n+1} = \mathbf{v}_n + (1-\gamma)\Delta t\mathbf{a}_n + \gamma\Delta t\mathbf{a}_{n+1}, \tag{36}$$

in which α_m, α_f, β, and γ are the algorithm parameters determined by the numerical dissipation parameter; $\Delta t = t_{n+1} - t_n$ is the time step; $\mathbf{d}_n$, $\mathbf{v}_n$ and $\mathbf{a}_n$ are approximations to $\mathbf{T}(t_n)$, $\dot{\mathbf{T}}(t_n)$ and $\ddot{\mathbf{T}}(t_n)$ respectively. Since equation (34) is a non-linear vector equation and the longitudinal and the transverse displacements are coupled with each other, a non-linear equation solver, e.g., the Newton–Raphson method, should be applied in order to update the displacement, velocity and acceleration vectors.

The dynamic responses of the transverse displacement of a point on the centreline of the pipe are computed from equations (34)–(36), when the external transverse load $p(x, t)$ given by a harmonic excitation with a frequency Ω and constant amplitude P_0, namely, $p(x, t) = P_0 \sin \Omega t$. In this paper, all the dynamic responses are computed when $P_0 = 1{\cdot}0$ N/m and $\Omega = 24\pi$ rad/s. The associated fluid velocity profile is shown in Figure 3, in which the dimensionless fluid velocity $\bar{U}$ increases linearly from zero to a constant value during 0·5 s, and then the velocity remains constant after it reaches the constant value. For numerical calculation, the numbers of the basis functions and the time step size are selected as $N = 5$ and $\Delta t = 0{\cdot}001$ s respectively.

In order to check the stability results given in Figure 2, it is required to investigate the dynamic responses for the linearized version of equation (34). The computed time histories of the transverse displacement of the linear model at $x = L/2$ are plotted in Figure 4. Figure 4(a) shows the dynamic response of the transverse displacement when the fluid velocity is zero. On the other hand, Figures 4(b)–(4d) demonstrate the time responses of the transverse displacements for the velocity profiles corresponding to $\bar{U} = 5$, $\bar{U} = 8$ and $\bar{U} = 10$ in Figure 3 respectively. As shown in Figures 4(a) and 4(b), when $\bar{U} = 0$ or 5, the dynamic responses are stable. The stable responses are coincident with the stability implied by Figure 2, where the real parts of the eigenvalues are zero. However, when $\bar{U} = 8$, the dynamic response exhibits the divergence instability. As shown in Figure 4(c), the response diverges without fluctuation. On the other hand, the response for $\bar{U} = 10$ blows out with fluctuation. In other words, the flutter instability is observed when $\bar{U} = 10$. These results can be confirmed by Figure 2, which illustrates that the first mode has pure real eigenvalues when $\bar{U} = 8$ while the first and second modes have eigenvalues with the real and imaginary parts when $\bar{U} = 10$.

Now, compare the dynamic responses for the non-linear model proposed in this paper with those for other non-linear models. This paper deals with comparisons only between the

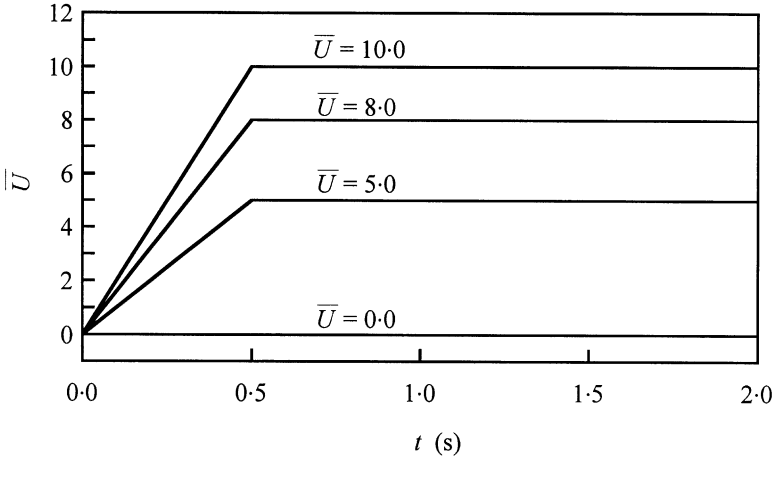

Figure 3. Fluid velocity profiles in the pipe.

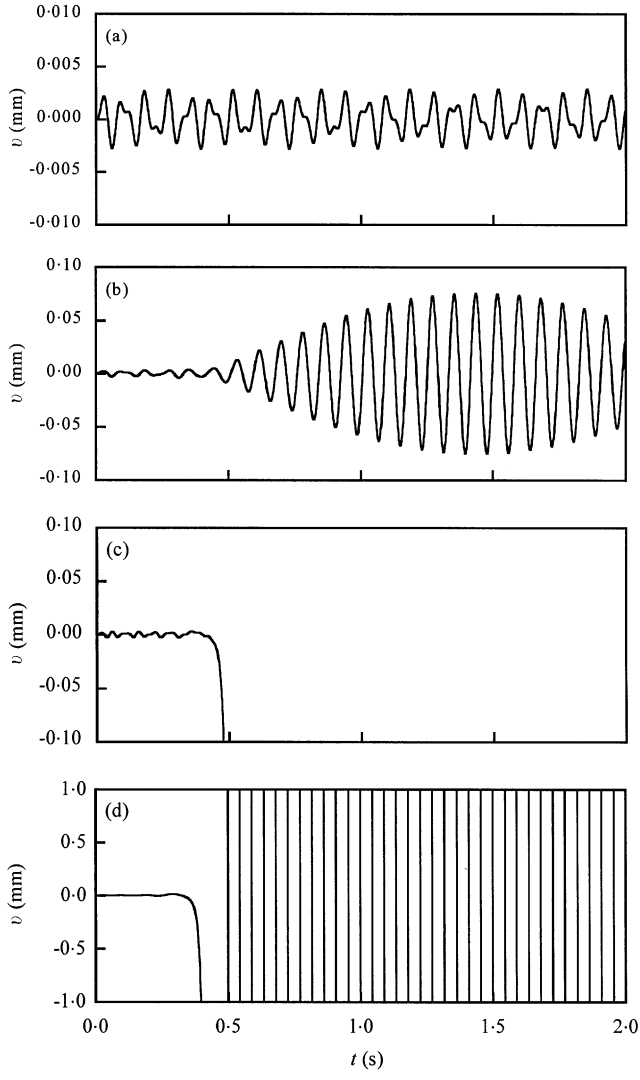

Figure 4. Dynamic responses of the transverse displacements for the linear model at $x = L/2$ when the fluid velocity is given by the profile corresponding to (a) $\bar{U} = 0{\cdot}0$, (b) $\bar{U} = 5{\cdot}0$, (c) $\bar{U} = 8{\cdot}0$ and (d) $\bar{U} = 10{\cdot}0$ in Figure 3.

new model and Païdoussis' model [1, 6]. The equations presented by Païdoussis are also discretized by using the same basis functions given in equation (20), and the dynamic responses are computed by using the generalized-α method with the same parameters and material properties. First, consider the dynamic responses of the transverse displacement when the fluid has no velocity, that is, $\bar{U} = 0$. In this case, although the new model and Païdoussis' model have different non-linear terms, as seen in equations (15), (16), (18) and (19), Figure 5 shows that, when $\bar{U} = 0$, there is no difference in the dynamic responses obtained from these two models. However, when the fluid velocity is non-zero, these dynamic responses become quite different from each other, as illustrated in Figure 6. This shows that the response for Païdoussis' model has a longer period and smaller amplitude compared to that for the new model. Recall that the proposed equations are derived consistently by only assuming linearized stress; however, Païdoussis' equations are derived by using the order-of-magnitude approximation and the infinitesimal strain theory.

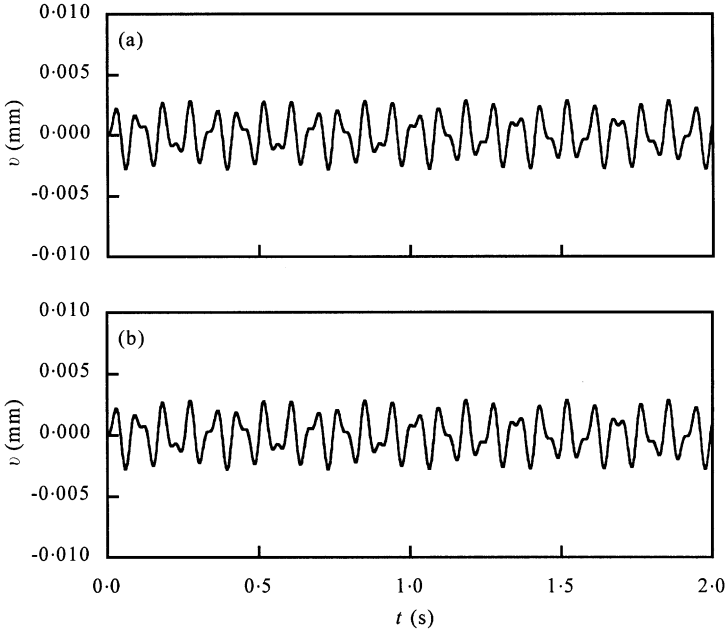

Figure 5. Dynamic responses of the transverse displacements for the non-linear model at $x = L/2$ when the fluid velocity is zero: (a) the new model; and (b) Païdoussis' model.

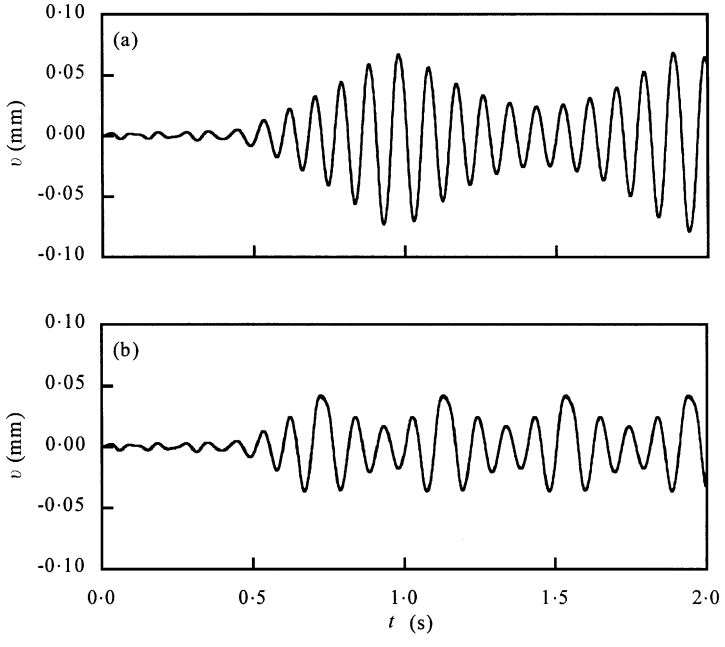

Figure 6. Dynamic responses of the transverse displacements for the non-linear model at $x = L/2$ when the fluid velocity is given by the profile corresponding to $\bar{U} = 5{\cdot}0$ in Figure 3: (a) the new model; and (b) Païdoussis' model.

Therefore, the proposed model is more reasonable than Païdoussis' model. This means that the presented theory can describe the coupled non-linear motion for the longitudinal and transverse displacements more accurately in comparison with Païdoussis' theory.

6. CONCLUSIONS

A new non-linear model is presented to analyze the vibration of a straight pipe conveying fluid when both ends are fixed. Using the Euler–Bernoulli beam theory and the general Lagrange strain, from the extended Hamilton principle the non-linear equations of motion for the longitudinal and transverse displacements are derived, where the longitudinal and transverse displacements are coupled with each other. With the discretized equations obtained by the Galerkin method, the natural frequencies and the dynamic responses are computed. Furthermore, the computation results from the proposed modelling are compared with those from Païdoussis' modelling.

The proposed model is more reasonable than Païdoussis' model, because the proposed equations are derived consistently by only assuming linearized stress while Païdoussis' equations are derived by using the order-of-magnitude approximation and the infinitesimal strain theory. On the other hand, it is observed that the dynamic responses, computed from the proposed non-linear theory, have the divergence instability for $6{\cdot}28 < \bar{U} < 8{\cdot}99$ and the flutter instability for $\bar{U} > 8{\cdot}99$.

ACKNOWLEDGMENT

This study was supported by the Brain Korea 21 Project of the Ministry of Education, Republic of Korea. This support is gratefully acknowledged.

REFERENCES

1. M. P. PAÏDOUSSIS 1998 *Fluid–Structure Interactions, Vol.* 1: *Slender Structures and Axial Flow*. San Diego, CA: Academic Press Inc.
2. A. L. THURMAN and C. D. MOTE 1969 *Journal of Engineering for Industry* **91**, 1147–1155. Non-linear oscillation of a cylinder containing flowing fluid.
3. C. DUPUIS and J. ROUSSELET 1992 *Journal of Sound and Vibration* **153**, 473–489. The equations of motion of curved pipes conveying fluid.
4. U. LEE, C. H. PAK and S. C. HONG 1995 *Journal of Sound and Vibration* **180**, 297–311. The dynamics of a piping system with internal unsteady flow.
5. D. G. GORMAN, J. M. REESE and Y. L. ZHANG 2000 *Journal of Sound and Vibration* **230**, 379–392. Vibration of a flexible pipe conveying viscous pulsating fluid flow.
6. C. SEMLER, G. X. LI and M. P. PAÏDOUSSIS 1994 *Journal of Sound and Vibration* **169**, 577–599. The non-linear equations of motion of pipes conveying fluid.
7. C. SEMLER and M. P. PAÏDOUSSIS 1996 *Journal of Fluids and Structures* **10**, 787–825. Non-linear analysis of the parametric resonances of a planar fluid-conveying cantilevered pipe.
8. Y. C. FUNG 1977 *A First Course in Continuum Mechanics*. Englewood Cliffs, NJ: Prentice-Hall Inc.
9. D. B. MCIVER 1972 *Journal of Engineering Mathematics* **7**, 249–261. Hamilton's principle for systems of changing mass.
10. J. CHUNG and G. M. HULBERT 1993 *American Society of Mechanical Engineers Journal of Applied Mechanics* **60**, 371–375. A time integration algorithm for structural dynamics with improved numerical dissipation: the generalized-α method.
11. J. CHUNG, N.-C. KANG and J. M. LEE 1996 *KSME International Journal* **10**, 138–145. A study on free vibration of a spinning disk.
12. J. CHUNG, C. S. HAN and K. YI 2001 *Journal of Sound and Vibration* **240**, 733–746. Vibration of an axially moving string with geometric non-linearity and translating acceleration.
13. R. D. BLEVINS 1979 Formulas for Natural Frequency and Mode Shape. New York: Van Nostrand Reinhold.